Scaling of the Scrape-Off Layer parameters in FTU tokamak

B. VIOLA[1], V. Pericoli Ridolfini[1], G. Maddaluno[1], G. Artaserse[1], F. Belli[1], W. Bin[2], L. Boncagni[1], L. Gabellieri[1], D. Marocco[1], C. Mazzotta[1], G. Pucella[1] and FTU Team*

[1] *Associazione ENEA sulla Fusione, Frascati (Rome), Italy*

[2] *Istituto di Fisica del Plasma C.N.R., Milan, Italy*

Introduction

Understanding how transport in the scrape-off layer (SOL) is affected by macroscopic and local parameters and how it is linked to heat transport on limiter/divertor tokamaks is still under debate. Usually experimental measurements of the SOL heat-flux decay length is carried out by means of infrared thermography [1], but since this diagnostic is not available in the Frascati Tokamak Upgrade (FTU) in this contribution the SOL of FTU in the magnetic configuration generated by a TZM (Molybdenum) toroidal limiter is studied by two arrays of reciprocating Langmuir probes. Despite being a limiter tokamak FTU results will help studying the amount and the spatial distribution of the energy and particle fluxes and can be applied to divertor machines before X-point formation and far from the X-point where the transport in the SOL is expected to be quite similar. This paper will present the results of a multi parameter SOL scaling carried out during the 2012 experimental campaign.

Experimental set-up

FTU characterizes as a medium size high-field/high density tokamak [2] with major radius $R_0 = 0.935m$, minor radius $a = 0.3m$, an average high ohmic power density $> 1.5MW/m^3$ and a wide range of main plasma parameters. Additional radio frequency plasma heating is possible. The parameter space explored in this work is bounded within the following ranges: plasma current ranging from 250kA up to 500kA, toroidal field ranges from $2.66T$ up to $7.5T$; the q_{cyl} safety factor varied between 3.5 and 14, Fig. 1. A density scan from 0.3×10^{20} to $1.3 \times 10^{20} m^{-3}$ at constant q_{cyl} and a magnetic field scan at constant current and density was performed. During the experiment the plasma column was kept to lay on the internal toroidal limiter to resemble the ITER start-up phase in order to contribute to the definition of the still uncertain value of the heat flux e-folding length in that phase. The poloidal limiter sector on the low field side was moved outwards by $1cm$, leaving the first $3cm$ of SOL depth free from any obstacle, Fig. 2. All the plasma discharges were ohmic and the measurements were carried out with two reciprocating probes located 180° poloidally away from each other. One is located

*See the appendix of P. Buratti et al., Proceedings of the 24th IAEA Fusion Energy Conf., San Diego, USA, 2012.

- 23 plasma ohmic discharges
- 2.66T < B_T < 7.54T
  - 2 discharges @ 2.66T
  - 2 " @3.55T
  - 6 " @4T
  - 6 " @5.55T
  - 3 " @6.4T
  - 4 " @7.54T
- 3 < q_{cyl} < 12
- 250kA < I_p < 500kA
- 0.27x10^{20} < $\overline{n_e}$ < 1.23x10^{20} [m^{-3}]

Fig. 1: Explored parameter space

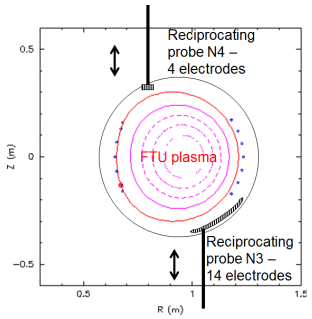

Fig. 2: Experimental set-up (not in scale)

outboard, $\sim 65^\circ$ below the equatorial plane, spanning nearly 30° from the vacuum vessel axis; the other is located inboard, $\sim 135^\circ$ above the equator, spanning nearly 8°. The movements of these probes have reached the last closed magnetic surface (LCMS) for most of the discharges. A detailed magnetic map of the SOL derived by equilibrium reconstruction allows identifying all the relevant magnetic surfaces and the values of the connection length L_{con}. For each probe, $n_e(r)$ and $T_e(r)$ are derived by a complete fit of the I (collected current) vs. V (applied voltage) characteristic, repeated at a frequency $\nu \sim 500Hz$. From them the particle flux (i.e. the ion saturation current) $I_{sat} \propto n_e \times T_e^{1/2}$ and the quantity $n_e \times T_e^{3/2}$ proportional to the power density flow P_{flow} are computed. As usual, the ion temperature is assumed equal to the electron one. The radial variation of all these quantities is then fitted with a model that foresees an exponential decay from the value at LCMS. The radial variation of the e-folding decay length due to the variation of L_{con} is also considered. The latter, in turn, is caused by the mismatch between the elliptical shape of the magnetic surfaces and the circular vessel, by the shift in their respective centres and by the presence of the poloidal limiter. The values of each quantity at LCMS and of its e-folding decay length, λ, are derived from this fitting procedure. The position of each probe in the vessel is carefully marked by determining when they come flush to the walls, i.e. when the collected signal emerges from the background noise. The values of the minor radius are mapped onto the outer equator, following the magnetic field line originating from the instantaneous probe position. The estimated error in the average radial position is $\pm 1mm$.

Results

Once the plasma column was in the desired position with a controlled elongation $\kappa \sim 1.07$, the probes, during the flattop of the current, moved out of their rest position behind the vessel walls and were swept inside the plasma for about 700ms. To obtain solid results from the analysis we adopted quite stiff criteria in selecting and handling the data. The quality and reliability of each piece of data eligible for the analysis has been singularly checked carefully. The errors (not shown here) on the measurements are in the order of $\pm 0.05 \times 10^{19} m^{-3}$ for the electron density and $\pm 4eV$ as for the electron temperature. Fig. 3 shows the electron density $n_{e,LCMS}$ and

temperature $T_{e,LCMS}$ at the LCMS plotted against the electron line average density $\overline{n_e}$ for three different sets of q_{cyl}. The considered values of $\overline{n_e}$ are time averaged in the sweeping window of the probe while $n_{e,LCMS}$ and $T_{e,LCMS}$ are poloidally averaged over the bottom array. The trend is clear: for $q_{cyl} < 5$ the density at the LCMS increases with $\overline{n_e}$, whereas for higher q_{cyl}, n_e and T_e show an increase at low density and then saturate as $\overline{n_e}$ is further increased. The reason of this saturation is presently under investigation and possibly is due to the density peaking factor. At low q_{cyl} values there is a dependence of the temperature with $\overline{n_e}$ which, we believe, is due to the increasing coupling of the electrons with the ions that are usually hotter inside the SOL. Conversely, at higher q_{cyl} the ion electron coupling should be already good at low density due to their longer dwell time in the SOL and hence longer L_{con}. Consistently, T_e is higher at low density and tend to decrease with $\overline{n_e}$, possibly because of the increase of the number of charge carriers, confirmed by greater values of λ_n, i.e. faster transport.

Fig. 3: $n_{e,LCMS}$ and $T_{e,LCMS}$ vs. ($\overline{n_e}$) for three different sets of q_{cyl}

Our equipment has allowed also to search for poloidal asymmetries of the SOL that we only outline here, due to the limited available space. We observe a general trend for both n_e and T_e to increase moving outboards from the lowest probe, located at the vessel axis, up to values twice higher on the upper inner probe array. The reason is being investigated, but we note its consistency with the upwards directed ion drift, driven by the magnetic field curvature and by $\nabla|B|$ [3]: future experiments with reversed toroidal field will confirm or not this point of view. Fig. 4 shows the electron density at the LCMS normalized to the value of the first electrode of the lower probe ($n_{e,LCMS}/n_{e,LCMS-e301}$) plotted as a function of the poloidal angle for different values of B_T: as for the lower probe its value increases moving counter-clockwise. In view of adding information to predict the flow channel's width for ITER during the pre X-point formation phase we searched for an empirical dependence of λ_q on the main macroscopic plasma parameters. An experimental regression analysis is applied to the FTU data taking as regression parameters: B_T, power crossing the LCMS (P_{SOL}), line averaged electron density $\overline{n_e}$ and plasma current I_p; elongation and plasma radius were not considered as in [1] because they were always the same. A least square fitting was applied to derive a parametric dependency:

$$\lambda_q(cm) = 0.819\, B_T^{0.0268}(T)\, I_p^{0.591}(MA)\, \overline{n_e}^{0.0508}(\times 10^{20} m^{-3})\, P_{SOL}^{-0.81}(MW) \qquad (1)$$

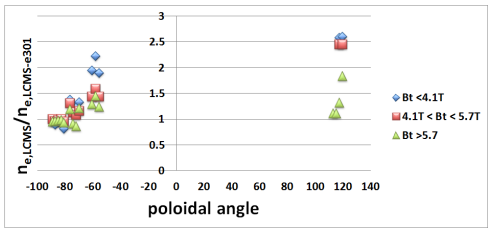

Fig. 4: $n_{e,LCMS}/n_{e,LCMS-e301}$ plotted as a function of the poloidal angle for different values of B_T

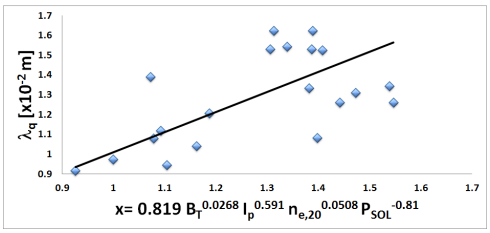

Fig. 5: Multi parameter regression

The main finding is a strong dependency on the plasma current and power crossing the LCMS; little dependency on the line averaged electron density was found. As Fig. 5 shows, the regression is not very satisfactory, probably due to lack of data. The recently proposed scalings [1] [4] would predict for FTU $\lambda_q \sim 3mm$ which is ~ 4 times lower than the values here reported.

Conclusions

The FTU SOL has been sampled with a couple of Langmuir probe arrays over a rather wide region of the operating parameter space in order to get data for determining reliable scaling laws: these results can be important not only for predicting the ITER SOL behaviour during the pre X-point phase, but can also contribute to understand the general behaviour of the main SOL. In addition to density and temperature we estimated from Langmuir probes data the heat-flux e-folding length λ_q, founding higher values than predicted from other scalings. Modelling of such results with a 2D code is underway as well as the analysis of the SOL turbulence data that have been collected simultaneously, in order to search for correlations with particle and energy transport. Strong poloidal asymmetries were also found on FTU plasmas for which two possible causes, namely the up or down particle drift and the pinch associated with the trapped particles are being investigated.

Acknowledgments

This work, supported by the Euratom Communities under the contract of Association between EURATOM/ENEA, was carried out within the framework the European Fusion Development Agreement. The views and opinions expressed herein do not necessarily reflect those of the European Commission.

References

[1] T. Eich et al., J. Nucl. Mat. 438 (2013) S72-S77.

[2] C. Gormezano et al., Fusion Sci. Technol., 2004, 45, 297-302.

[3] Wesson J. 1997 Tokamaks, 2nd edn.

[4] Scarabosio et al., J Nucl. Mat. 438 (2013) S426-S430.